This study investigates a grinding process in a tumbling mill loaded by impact, crushing, and abrasion. The impact, compression, and shear interactions of particles are taken into account, the intensity of which is determined by the zones of flight, shear layer, and solid flow of the fill in the cross-section of the rotating drum chamber.

The task addressed is to determine the influence of rotation speed on the energy intensity of the grinding process for individual loading mechanisms.

An experimental method for numerical modeling of productivity analogs for grinding mechanisms by the energies of the corresponding interactions was applied.

The energy intensity of the process was estimated by the ratios of productivity analogs and the relative power of rotation drive. Energy efficiency was determined taking into account experimental data on physical productivity and drive power of the mill model.

The effect of rotation speed on grinding was experimentally estimated at a chamber filling degree of 0.45.

The phenomenon of an intensive decrease in the energy intensity of the grinding process with a decrease in rotation speed was established.

The results made it possible to identify energy-efficient values of the relative rotation speed for the grinding processes: coarse – by impact at $\psi_\omega = 0.75–0.9$, medium – by crushing at $\psi_\omega = 0.55–0.65$, and fine – by abrasion at $\psi_\omega = 0.3–0.4$. The established effect is explained by the revealed activation of interactions: impact – at high-speed, compressive – at medium-speed, and shear – at low-speed rotation.

The established patterns enable prediction of rational technological parameters for energy-saving processes of multi-stage grinding in tumbling mills

Keywords: tumbling mill; intra-chamber filling; grinding by impact, crushing, and abrasion; energy efficiency

UDC 621.926.5:539.215
DOI: 10.15587/1729-4061.2025.343388

DETERMINING THE EFFECT OF ROTATION SPEED ON THE ENERGY EFFICIENCY OF THE IMPACT, COMPRESSION, AND ABRASION GRINDING PROCESSES IN A TUMBLING MILL

Yuriy Naumenko
Corresponding author
Doctor of Technical Sciences, Professor
Department of Construction, Road and Reclamation Machines
National University of Water and Environmental Engineering
Soborna str., 11, Rivne, Ukraine, 33028
E-mail: informal9m@i.ua

Kateryna Deineka
PhD, Teacher of the Highest Category
Separate Structural Unit "Rivne Technical Vocational College of the National University of Political Science and Technology"
Vyshyvanka str., 35, Rivne, Ukraine, 33027

Received 25.08.2025
Received in revised form 03.11.2025
Accepted 10.11.2025
Published 30.12.2025

How to Cite: *Naumenko, Y., Deineka, K. (2025). Determining the effect of rotation speed on the energy efficiency of the impact, compression, and abrasion grinding processes in a tumbling mill. Eastern-European Journal of Enterprise Technologies, 6 (1 (138)), 41–53. https://doi.org/10.15587/1729-4061.2025.343388*

1. Introduction

Grinding in tumbling mills is a rather energy-intensive technological process [1]. High energy intensity is caused by intensive energy dissipation due to frictional circulation of the internal chamber loading. Given the wide application of such grinders, the task to improve their energy efficiency remains relevant [2].

The recently reported modeling results do not make it possible to reveal the relationship between the drive power and the productivity of the grinding process [3]. The prediction task is complicated by the simultaneous combination of the action of several loading mechanisms of the granular medium in the chamber of the rotating drum, which enable implementation of the mechanisms of destruction of the crushed material by breaking, crushing, and abrasion [4–7]. In addition to the basic loading mechanisms by impact and shear [4, 5], an intermediate compression mechanism is taken into account [6, 7]. The determining factor in the implementation of the loading mechanisms is the rotation speed of the loaded drum [7]. It is believed that at increased speed, the impact load increases, which enables coarse grinding. Instead, a decrease in speed initially leads to compression of the load, which provides medium grinding, and with a further decrease – to shear, which provides fine grinding.

The influence of rotation speed on the loading and destruction mechanisms underlies the application of two- [8] and three-stage [9] grinding processes in tumbling mills. The two-stage process consists of a sequential transition from a short-term high-speed first stage of coarse grinding mainly by impact to the subsequent long-term low-speed second stage of fine grinding mainly by shear. The three-stage process is supplemented by an intermediate second stage of medium grinding mainly by compression.

However, the quantitative results of the influence of rotation speed on grinding when implementing different loading mechanisms remain unknown, which limits the functionality of the equipment and does not contribute to solving the task of reducing the energy intensity of the process.

Given the above, the problem of establishing the influence of rotation speed on the energy efficiency of grinding in

a tumbling mill by impact, compression, and shear appears to be rather relevant.

2. Literature review and problem statement

Experimental studies on the qualitative influence of rotation speed on the resistance of the tumbling mill drive were reported in [10–14]. In work [10], an increase in the drive power for wet grinding was established with an increase in the relative rotation speed in the range $\psi_\omega = 0.65–0.85$. Similar results were obtained in [11] for wet grinding and in [12] for dry grinding of copper ore at $\psi_\omega = 0.6–0.85$, as well as in [13] for wet grinding of iron ore at $\psi_\omega = 0.6–0.8$. In work [14], based on experiments and modeling by the DEM method, it was established that with an increase in the rotation speed in the range $\psi_\omega = 0.6–1$, the moment and power of rotation resistance first increase and then decrease.

A decrease in the energy intensity of wet grinding of potash ore in a rod tumbling mill to 25% with a decrease in the rotation speed in the range $\psi_\omega = 0.5–0.8$ was experimentally found in [15].

However, quantitative characteristics of the influence of rotation speed on the drive parameters were not established in [10–15].

A fairly large body of research [16–33] considers establishing a rational value of the rotation speed when achieving the overall maximum productivity and minimum energy intensity of the grinding process in a tumbling mill. However, the reported results are characterized by a significant spread of numerical values.

Thus, papers [16–22] consider identifying the rational value of the speed when achieving maximum productivity. Increased values of the speed $\psi_\omega = 0.7–0.85$ were identified as rational in terms of productivity. The rational value $\psi_\omega = 0.85$ was experimentally established in [16] in the studied range $\psi_\omega = 0.7–0.85$ for dry grinding of limestone and clinker, as well as in work [17] in the range $\psi_\omega = 0.65–0.85$ for dry grinding of pumice. The rational value $\psi_\omega = 0.7–0.8$ was numerically established in [18] in the considered range $\psi_\omega = 0.5–0.9$ for wet grinding of platinum ore based on the generalization of the array of experimental data. A similar value was numerically found by the DEM method in [19] in the range $\psi_\omega = 0.5–1$, and also experimentally established in [20] in the range $\psi_\omega = 0.7–0.8$ for wet grinding of copper ore. The rational value of $\psi_\omega = 0.75$ in terms of the maximum thermodynamic heating temperature was numerically found by the DEM method with experimental verification in [21] in the studied range $\psi_\omega = 0.55–0.95$ for dry grinding of iron ore. The rational value of $\psi_\omega = 0.7$ was experimentally found in [22] in the range $\psi_\omega = 0.6–0.85$ for dry grinding of calcite. The uncertainty and unfoundedness of the wide range of recommended speed values is due to the neglect of the differentiated influence of different loading mechanisms on the grinding process.

Studies [23–33] consider finding the rational value of the rotation speed when achieving the minimum energy intensity.

In [23–25], the average values of the speed $\psi_\omega = 0.55–0.6$ were established as rational in terms of energy intensity. The rational value $\psi_\omega = 0.6$ was experimentally established in [23] in the studied range $\psi_\omega = 0.2–0.7$ for wet grinding of iron ore. The rational value $\psi_\omega = 0.55$ was experimentally found in [24] in the studied range $\psi_\omega = 0.5–0.9$ for dry grinding of quartz, limestone, and cement clinker, as well as in work [25] in the range $\psi_\omega = 0.55–0.7$.

In [26–30], reduced values of rotation speed $\psi_\omega = 0.3–0.4$ were found to be rational. The rational value $\psi_\omega = 0.4$ was established based on the application of a numerical empirical model in work [26] in the considered range $\psi_\omega = 0.4–0.9$ for wet grinding of platinum ore. The value $\psi_\omega = 0.4$ was found based on the application of the numerical method of the achievable region in [27] in the same ψ_ω range for wet grinding of gold-bearing ore. The rational value $\psi_\omega = 0.4$ was found based on the application of a numerical mathematical model of an open cycle of grinding in [28] for wet grinding of platinum ore. The value $\psi_\omega = 0.4$ was also established in the review of the application of the numerical method of optimization of the achievable region in [29] for wet grinding in a tumbling mill. The rational value of $\psi_\omega = 0.3–0.4$ was established experimentally in [30] in the studied range of $\psi_\omega = 0.2–0.5$ for dry grinding of platinum ore. An increase in the productivity of the grinding process with an increase in the rotation speed and a decrease in energy consumption with a decrease in the speed were found. Unsolved questions, reasons for the unsolved ones?

In [31–33], low values of the rotation speed of $\psi_\omega = 0.03–0.1$ were found to be rational. The rational value of $\psi_\omega = 0.1$ was numerically established by the DEM method in [31] in the studied range of $\psi_\omega = 0.1–0.53$ for dry grinding of iron ore. At $\psi_\omega = 0.1$, the highest intensity of the grinding process was found. The rational value of $\psi_\omega = 0.04$ was experimentally established in [32] in the considered range of $\psi_\omega = 0.04–0.55$ for dry grinding of quartz sand. The rational value of $\psi_\omega = 0.03$ was experimentally established in [33] in the range of $\psi_\omega = 0.03–0.37$ for the last stage of dry two-stage grinding of quartz sand.

However, the quantitative characteristics of the impact on the productivity and energy intensity of grinding in a tumbling mill and the rational values of the rotation speed for individual mechanisms of impact, compression, and shear loading were not established in [16–33].

The dynamic parameters of the impact, compression, and shear interaction of the elements of the granular loading of the rotating drum chamber are determined by the characteristics of the zones of movement of the medium. The behavior of these zones was modeled by the analytical and experimental method. In [34], the position of the boundary of the transition between the solid zone and the flight zone was established. In [35], the characteristics of the shear layer zone were revealed. In [36], a general calculation algorithm for modeling zones in the loading motion pattern was developed. However, the results did not provide for a differential assessment of the speed parameters of the processes of impact, contact, and shear grinding. The characteristics of the active zones of loading motion were studied in [37–41] by the visualization method. The dynamics of the self-oscillating action of the loading and the grinding characteristics for discrete filling of the chamber were evaluated in [37]. In [38], the influence of the degree of filling of the chamber on self-oscillating grinding for a discrete content of the crushed material in the loading was considered. The influence of material content on the modes of motion of the loading and self-oscillating grinding for discrete filling of the chamber was studied in [39]. In [40], the influence of simultaneous changes in filling and material content on grinding was studied. The mathematical mechanism of loss of stability of the flow of polygranular loading in the chamber of a rotating drum was revealed in [41]. In [42], qualitative conditions for the stability of the dynamic system of a tumbling mill were established. However, the results reported in [37–42] correspond only to the self-oscillating mode of behavior of the intra-chamber loading.

To determine the parameters of impact, compression, and shear interaction, an experimental method of numerical modeling was used based on visualization of data on the behavior of granular loading in the chamber of a rotating drum [43–45]. A mathematical model of the mechanism of destruction by crushing under the action of the impact loading mechanism was built in [43]. In [44], a model of the mechanism of destruction by crushing under the action of the compression loading mechanism was constructed. A model of the mechanism of destruction by abrasion under the action of the shear loading mechanism was synthesized in [45]. The influence of kinematic parameters and mass fractions of the loading motion zones on the productivity was taken into account. However, the results relate to productivity only for individual loading mechanisms and do not allow us to assess the influence of each of them on the energy intensity of the grinding process integrated by the mechanisms when the rotation speed changes.

Our review of the literature [1–45] allowed us to draw a conclusion regarding the essence of the unsolved problem. It relates to the absence of models for predicting the differential effect of rotation speed on the energy efficiency of qualitatively different grinding processes in a tumbling mill by impact, compression, and shear. This is due to the difficulties of analytical and numerical modeling and the complexity of instrumental experimental research of the effect of rotation speed on grinding when implementing various loading mechanisms. The impossibility of applying such models is especially negatively manifested in the case of implementing an energy-saving process of multi-stage grinding.

The above considerations indicate the relevance of conducting a study on the effect of rotation speed on the energy intensity of grinding for individual destruction mechanisms.

3. The aim and objectives of the study

The aim of our work is to establish the influence of rotation speed on the technological and energy parameters of the grinding process in a tumbling mill when implementing the loading mechanisms in the intra-chamber loading by impact, compression, and shear. This will make it possible to predict the energy efficiency of the grinding process by implementing different mechanisms of destruction of the crushed material when varying the rotation speed.

To achieve this goal, the following tasks were set:

– to model experimentally the productivity of the grinding process in a tumbling mill for different rotation speeds;

– to model experimentally the energy intensity of the tumbling mill rotation drive for different rotation speeds;

– based on numerical results, to identify the qualitative influence of rotation speed on the total energy intensity of the grinding process;

– based on numerical results from data visualization, to identify the comparative qualitative influence of rotation speed on the energy intensity of the grinding process for the loading mechanisms by impact, contact, and shear.

4. The study materials and methods

4. 1. The object and hypothesis of the study

The object of our study is the grinding process in a tumbling mill when implementing individual loading mechanisms in intra-chamber loading. The subject of the study is mathematical modeling of dependences of the specific productivity and energy intensity of grinding processes on the rotation speed when implementing the mechanisms of impact, compression, and shear loading, which enables implementation of the mechanisms of destruction by breaking, crushing, and grinding.

Underlying the models of the considered grinding mechanisms are the relative dynamic parameters of the impact, compression, and shear interaction of the elements of the granular fill, which are the criteria for the similarity of the movement of the fill and the grinding process. As analogs to the productivity of grinding processes in a tumbling mill by breaking, crushing, and grinding, the energies of the impact, compression, and shear interaction are taken [43–45].

It was assumed that the impact interaction of the loading elements takes place on the surface of the transition of the flight zone into the shear layer zone [43], the compressive interaction takes place on the surface of the transition of the shear layer into the solid zone [44], and the shear interaction takes place in the shear layer [45].

The interaction of the chamber with the fill was assumed mainly along a cylindrical surface. The influence of the end walls of the chamber on the movement of the fill was neglected.

The factors of parameters for the steady-state mode of the fill movement in the chamber of the rotating drum were considered to be stationary flow patterns.

It was assumed that the mode of motion of the fill in the chamber of the rotating drum is steady. The dependences of the torque and power of the drive resistance on the rotation speed were assumed to be quasi-static.

As a simplified case of monofractional loading of the chamber of the rotating drum, a granular material with spherical particles with a relative size $\psi_d = 0.0104$ was used. The value of the angle of internal friction of the material was 30°.

Since the boundary edge effect of the flow of the fill on the end wall of the chamber turned out to be insignificant, physical visualization of the data was adopted as a method of experimental research.

4. 2. Methodology for experimental modeling of the grinding process performance in a tumbling mill

The relative drum rotation speed ψ_ω was taken as the input parameter, which is a variable factor of the research

$$\psi_\omega = \omega\sqrt{\frac{R}{g}}, \quad (1)$$

where $\psi_\omega = \omega / \omega_{cr}$ – relative rotation speed, ω – current value of the angular velocity of rotation of the drum; $\omega_{cr} = \sqrt{g/R}$ – critical angular velocity of rotation of the drum, which corresponds to the equality of centrifugal acceleration on the cylindrical surface of the drum chamber $\omega^2 R$ to the acceleration of gravity g; R – radius of the cylindrical drum chamber. The value of relative velocity ψ_ω during the experimental determination of the productivity of the grinding process varied in the range of 0.15–0.85 with a step of 0.1.

A stroboscopic tachometer was used to measure the rotation speed.

As a geometric characteristic of the granular fill of the drum chamber, the degree of filling the chamber with the loading was taken – $\kappa = w / (\pi R^2 L)$, where w is the volume of the portion of the fill in the chamber at rest, L – length of the drum chamber.

The value of the degree of filling during all studies was taken as $\kappa = 0.45$, which corresponds to the grinding process

in a tumbling mill with high throughput in terms of output of the finished product.

As a geometric characteristic of the content of particles of crushed material in the grinding loading of the drum chamber, the degree of filling of the grinding loading with crushed material was taken – $\kappa_m = w_m / (\kappa\pi R^2 L)$, where w_m is the volume of a portion of crushed material in the chamber at rest. The value of the degree of filling of the grinding loading with crushed material in the experimental determination of the productivity of the grinding process was taken as $\kappa_m = 0.4$, which approximately corresponds to the value of the volume fraction of the gaps between spherical bodies of the same size at rest. Such content of crushed material in the fill corresponds to the process of coarse grinding in a tumbling mill.

Laboratory beakers were used to dose the loading portion. The portion volume was determined at rest.

As a geometric characteristic of the element of the granular fill of the drum chamber, the relative size of the element in the chamber was taken – $\psi_d = d / (2R)$, where d – average absolute size of the element. Steel balls with a relative size of $\psi_d = 0.026$ were used as grinding media in the experimental laboratory mill. Particles of pre-crushed cement clinker with a relative size of $\psi_{dm} < 0.0059$ were used as the grinding material.

A laser-type analyzer was used to measure the particle size of the fill.

Laboratory studies of the grinding process in a tumbling mill were based on standard methodologies. We determined the particle size distribution of the starting material and the finished grinding product by sieving them through sieves and calculating the fraction content.

The duration of the grinding process was 30 min.

The productivity of the grinding process in a tumbling mill was estimated by the value of sieving through control sieve No. 008. The relative productivity C was taken as a characteristic of productivity

$$C = 1 - \frac{m_r}{m_m}, \tag{2}$$

where m_r is the mass of the residue on sieve No. 008 after sieving, m_m is the total mass of the crushed material before sieving.

Electronic scales were used to measure the mass of the crushed material.

4. 3. Methodology for experimental modeling of the energy intensity of the tumbling mill drive

As a criterion for evaluating the power parameter of the tumbling mill drive, the relative moment of resistance of the load to rotation $\psi_M = M / M_{\max}$ is taken, where M is the absolute value of the moment of resistance, $M_{\max}$ is the value of the conditional maximum moment of resistance. The moment $M_{\max}$ corresponds to the imaginary distribution of the fill in the cross section of the chamber in the form of an ideal solid segment, rotated together with the drum relative to the initial position at rest at a right angle θ (Fig. 1).

The magnitude of the conditional maximum moment $M_{\max}$ is equal to the product of the load gravitational force modulus G by distance OC from the rotation axis O to the center of gravity C of imaginary segment 1 (Fig. 1)

$$M_{\max} = (2 / 3)R^3(\sin^3\beta)L\rho g,$$

where ρ is the bulk density of the fill at rest; β is half of the central angle of the ideal load segment in the cross-section of the chamber, the value of which is determined from equation $2\beta - \sin(2\beta) = 2\pi\kappa$.

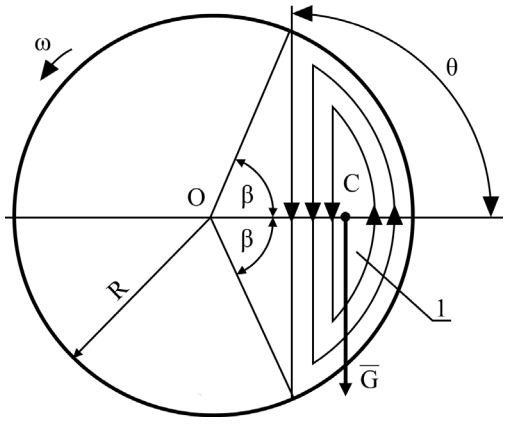

Fig. 1. Scheme of the occurrence of the conditional maximum moment of resistance of the flowing load to the rotation of the filled drum $M_{\max}$: 1 — imaginary ideal load segment in the cross-section of the chamber

To determine the absolute moment of resistance M, the calibration dependences of the drive torque on the rotation speed were used, which were obtained using a dynamometer.

As the power characteristic of the tumbling mill drive, the relative moment of resistance of the load to rotation when the chamber is half filled $\psi_{M0.5}$ was taken

$$\psi_{M0.5} = \frac{3}{2}\frac{M}{R^3 L\rho g}, \tag{3}$$

where $\psi_{M0.5} = M/M_{\max 0.5}$ – relative moment of resistance at half-filling, where $M_{\max 0.5} = (2/3)R^3 L\rho g$ – conditional maximum moment of resistance at half-filling, the value of which corresponds to the maximum possible value of $M_{\max}$ at $\kappa = 0.5$.

The relative power of the load resistance to rotation at half-filling of the chamber $\psi_{P0.5}$ is taken as the energy characteristic of the tumbling mill drive

$$\psi_{P0.5} = \psi_{M0.5}\psi_\omega. \tag{4}$$

The value of relative velocity ψ_ω during the experimental determination of $\psi_{M0.5}$ and $\psi_{P0.5}$ varied in the range of 0–1.35 with a step of 0.05.

4. 4. Methodology for numerical modeling of the total energy intensity of the grinding process in a tumbling mill

As characteristics of the total energy intensity of the grinding process in a tumbling mill, the total specific productivity C_E and the total specific energy intensity E_C of grinding were taken:

$$C_E = \frac{C}{\psi_{P0.5}}, \tag{5}$$

$$E_C = \frac{\psi_{P0.5}}{C}. \tag{6}$$

The ratio of process productivity C and rotational resistance power $\psi_{P0.5}$ was adopted as criteria for evaluating the total energy intensity of grinding.

4. 5. Methodology for numerical modeling of energy intensity of grinding processes by mechanisms of destruction by impact, crushing, and grinding

An experimental method of numerical modeling based on experimental visualization of the behavior of the fill in the chamber of a rotating drum was used to determine the parameters of shear interaction. The visualization was carried out by fixing through a transparent end wall and further processing of the patterns of the load movement in the cross section of the chamber. Separate obtained patterns of steady-state load movement in the chamber of a stationary rotating drum at $\kappa = 0.45$ [43] are shown in Fig. 2.

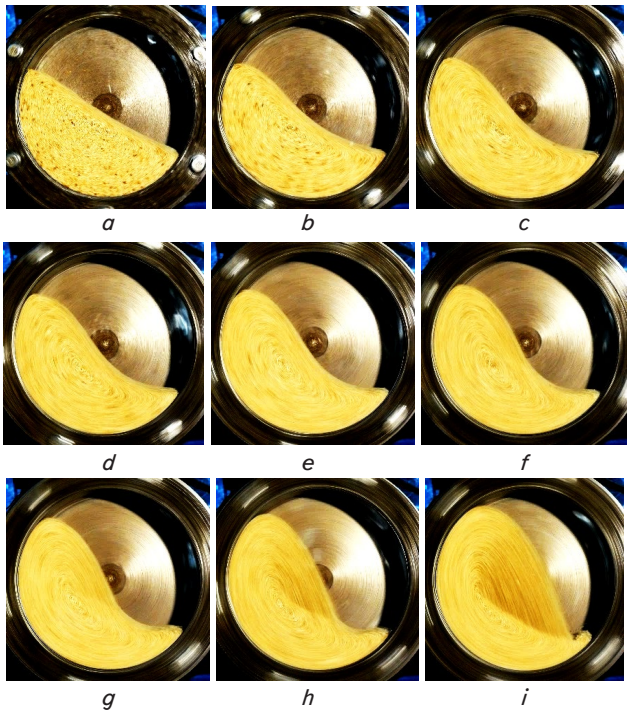

Fig. 2. Motion patterns of granular fill with relative particle size $\psi_d = 0.0104$ at chamber filling degree $\kappa = 0.45$: *a* – $\psi_\omega = 0.1$; *b* – $\psi_\omega = 0.2$; *c* – $\psi_\omega = 0.3$; *d* – $\psi_\omega = 0.4$; *e* – $\psi_\omega = 0.5$; *f* – $\psi_\omega = 0.6$; *g* – $\psi_\omega = 0.7$; *h* – $\psi_\omega = 0.8$; *i* – $\psi_\omega = 0.9$ (according to [43])

The algorithm for implementing the data visualization method involved sequentially implementing a number of stages [43–45]. A computational scheme of the three-phase mode of fill motion in the cross-section of a rotating chamber was applied (Fig. 3). According to the scheme, impact, compression, and shear interactions were determined by numerical modeling.

The simulation cycle by experimental visualization of data for one drum rotation speed consisted of the following stages:

1) obtaining a pattern of the fill motion for the current value of the drum rotation speed;

2) visualization of the fill motion zones by highlighting them in the pattern;

3) visualization of the central averaged normal cross-section of the shear layer by highlighting in the obtained pattern;

4) visualization of geometric data by measuring them in the pattern;

5) visualization of the loading dilatancy in the motion zones by evaluating them from the pattern;

6) calculation of values of the loading interaction parameters using the corresponding expressions;

7) obtaining a pattern of the loading motion for the next value of the drum rotation speed and transition to a new simulation cycle.

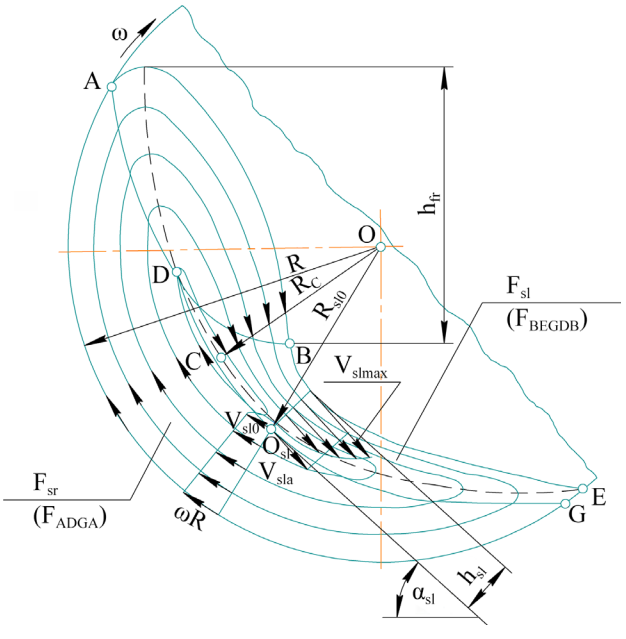

Fig. 3. Calculation diagram of the motion pattern with flow lines of granular fill in the chamber of a rotating drum (according to [43–45])

Measurements of the linear dimensions and areas of geometric figures in the motion patterns were carried out using specialized computer systems.

The value of the relative rotation speed ψ_ω when visualizing the fill motion patterns varied from the rest state to the boundary of the transition of the circulation mode of motion to the near-wall layer mode in the range of 0–1.35 with a step of 0.05.

As characteristics of the volumes of the solid zone, shear layer zone, and flight zone of the fill, the mass fractions of solid zone κ_{sr}, shear layer zone κ_{sl}, and flight zone κ_{fr} were taken:

$$\kappa_{sr} = \frac{F_{sr}}{\pi R^2 \kappa}, \tag{7}$$

$$\kappa_{sl} = \frac{F_{sl}}{\pi R^2 \kappa \upsilon_{sl}}, \tag{8}$$

$$\kappa_{fr} = 1 - \kappa_{sr} - \kappa_{sl}, \tag{9}$$

where F_{sr} is the area of the solid zone F_{ADGA} (Fig. 3) in the motion pattern; F_{sl} is the area of the shear layer zone F_{BEGDB}; υ_{sl} is the dilatancy of the shear layer zone.

As an analog of the productivity of the impact grinding process, the relative energy of the impact interaction of the loading elements is taken [43]

$$Q_i = \frac{h_{fr}}{4R} \kappa_{fr},$$

where h_{fr} is the vertical distance from the highest to the lowest point on the free surface of the loading flight zone in the motion pattern.

As an analog of the productivity of the crushing process, the relative energy of the compressive interaction of the loading elements is taken [44]

$$Q_c = \frac{\omega^2\left(R^2 - R_{sl0}^2\right)^2}{8h_{sl}^2 Rg}\kappa_{sl},$$

where R_{sl0} is the radial coordinate of the base of the central averaged normal cross-section of the shear layer; h_{sl} is the height of the central averaged normal cross-section of the shear layer.

The relative energy of the shear interaction of the loading elements is taken as an analog of the productivity of the grinding process by grinding [45]

$$Q_a = \frac{\left(V_{sl\max} + V_{sl0}\right)^2 R}{h_{sl}^2 g}\kappa_{sl},$$

where $V_{sl\max} = \sqrt{2W_i \cdot \sin\alpha_{sl} \cdot \frac{\cos\varphi}{1-\sin\varphi} \cdot h_{sl} - V_{sl0}^2}$ – maximum shear velocity in the central averaged normal cross-section of the shear layer; $V_{sl0} = \omega R_{sl0}$ – shear velocity of the support surface of the central averaged normal cross-section of the shear layer; R_{sl0} – radial coordinate of the base of the central averaged normal cross-section of the shear layer; α_{sl} – angle of inclination of the base of the averaged normal cross-section of the shear layer to the horizontal; φ – angle of internal friction of the granular load; $W_i = g + a_{fr} = \sqrt[3]{-L/2+\sqrt{f}} + \sqrt[3]{-L/2-\sqrt{f}} - q/3$ – apparent total vertical acceleration of the shear layer, which causes its movement; a_{fr} – apparent additional inertial acceleration of the shear layer due to the increase in kinetic energy after the impact interaction of the flight zone with the shear layer;

$$f = \left(-\frac{q^2}{9} + \frac{m}{3}\right) + \left(\frac{L}{2}\right),\ L = 2\left(\frac{q}{3}\right)^3 - \frac{qm}{3} - 2\frac{V_{sl0}^6}{d^3},$$

$$q = -\frac{1}{d^3}\left(\frac{V_{sla}^2}{c^2} + 3d^2V_{sl0}^2\right),\ m = \frac{1}{d^3}\left(2\frac{V_{sla}}{c}V_{sl0}^3 + 3dV_{slo}^4\right),$$

$$c = \frac{1-\sin\varphi}{3h_{sl}\sin\alpha_{sl}\cos\varphi} \text{ and } d = \frac{2h_{sl}\sin\alpha_{sl}\cos\varphi}{1-\sin\varphi} \text{ – variables;}$$

$V_{sla} = \frac{\omega\left(R^2 - R_{sl0}^2\right)}{2h_{sl}}$ – average value of the speed of movement in the central averaged normal section of the shear layer.

As characteristics of performance analogs, which are brought to a comparative form for further comparative analysis, normalized performance analogs of the processes of impact crushing Q_{in}, crushing Q_{cn}, and grinding Q_{an} are adopted:

$$Q_{in} = \frac{Q_i}{Q_{i\max}}, \quad (10)$$

$$Q_{cn} = \frac{Q_c}{Q_{c\max}}, \quad (11)$$

$$Q_{an} = \frac{Q_a}{Q_{a\max}}, \quad (12)$$

where $Q_{i\max}$, $Q_{c\max}$ and $Q_{a\max}$ are the maximum values of Q_i, Q_c and Q_a.

As characteristics of relative dimensionless analogs of productivity, which are transformed for further comparative quantitative analysis, taking into account the proportional influence of the values of the experimentally obtained dependences of absolute productivity on the rotation speed, generalized analogs of the productivity of the processes of impact grinding Q_{ig}, crushing Q_{cg} and grinding Q_{ag} are adopted:

$$Q_{ig} = Q_{in}C, \quad (13)$$

$$Q_{cg} = Q_{cn}C, \quad (14)$$

$$Q_{ag} = Q_{an}C. \quad (15)$$

As characteristics of the energy intensity of grinding processes in a tumbling mill when implementing individual loading mechanisms in intra-chamber loading, taking into account the influence of the values of the experimentally obtained dependences of the absolute drive power on the rotation speed, the following analogs of the specific productivity of grinding by impact Q_{Ei}, crushing Q_{Ec}, and grinding Q_{Ea} were adopted:

$$Q_{Ei} = \frac{Q_{ig}}{\psi_{P0.5}}, \quad (16)$$

$$Q_{Ec} = \frac{Q_{cg}}{\psi_{P0.5}}, \quad (17)$$

$$Q_{Ea} = \frac{Q_{ag}}{\psi_{P0.5}}, \quad (18)$$

and analogs of the specific energy intensity of the processes of impact grinding E_{Qi}, crushing E_{Qc}, and grinding E_{Qa}:

$$E_{Qi} = \frac{\psi_{P0.5}}{Q_{ig}}, \quad (19)$$

$$E_{Qc} = \frac{\psi_{P0.5}}{Q_{cg}}, \quad (20)$$

$$E_{Qa} = \frac{\psi_{P0.5}}{Q_{ag}}. \quad (21)$$

The ratio of generalized analogs of the productivity of impact grinding Q_{ig}, crushing Q_{cg}, and grinding Q_{ag} and the power of resistance to rotation $\psi_{P0.5}$ was adopted as criteria for assessing the energy intensity of grinding processes for destruction mechanisms.

5. Results of research on the processes of impact, crushing, and grinding in a tumbling mill

5. 1. Results of experimental modeling of the productivity of the grinding process in a tumbling mill

A plot of the results from the experimental determination of change in relative productivity C from the relative rotation speed ψ_ω is shown in Fig. 4. The values of C were calculated using expression (2), the values of ψ_ω were calculated using expression (1).

Our experimental dependence of the numerical values of relative productivity C characterizes the quantitative influence of the rotation speed on the overall productivity of the grinding process in the tumbling mill.

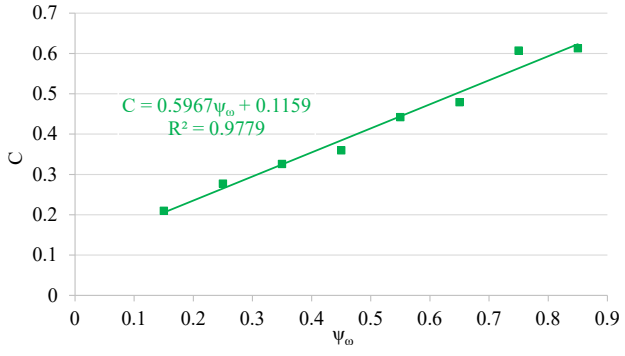

Fig. 4. Experimental dependence of change in relative productivity C on the relative rotation speed ψ_ω

5. 2. Results of experimental modeling of the energy intensity of the tumbling mill drive

Plots of our results from the experimental determination of change in the relative moment of the fill resistance to rotation when the chamber is half filled $\psi_{M0.5}$ and the relative power of the load resistance to rotation when the chamber is half filled $\psi_{P0.5}$ from the relative rotation speed ψ_ω are shown in Fig. 5. The values of $\psi_{M0.5}$ and $\psi_{P0.5}$ were calculated using expressions (3) and (4).

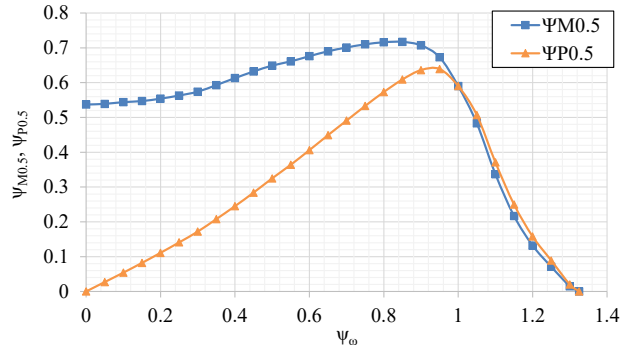

Fig. 5. Experimental dependence of change in the relative moment of load resistance to rotation at half-filling of the chamber $\psi_{M0.5}$ and the relative power of load resistance to rotation at half-filling of the chamber $\psi_{P0.5}$ on the relative rotation speed ψ_ω

The obtained experimental dependences of the numerical values of change in the relative moment of resistance $\psi_{M0.5}$ and the relative power of resistance $\psi_{P0.5}$ of the load to rotation at half filling of the chamber characterize the quantitative influence of the rotation speed on the energy intensity of the tumbling mill drive.

5. 3. Results of numerical modeling of the total energy intensity of the grinding process in the tumbling mill

A plot of our results from the numerical determination of change in the total specific grinding efficiency C_E from the relative rotation speed ψ_ω is shown in Fig. 6. The values of C_E were calculated from expression (5).

A plot of our results from the numerical determination of change in the total specific energy intensity of grinding E_C from the relative rotation speed ψ is shown in Fig. 7. The E_C values were calculated using expression (6).

The obtained functional dependences of the numerical values of change in the total specific productivity C_E and the total specific energy intensity E_C of grinding characterize the quantitative influence of the rotation speed on the total energy intensity of the grinding process in a tumbling mill.

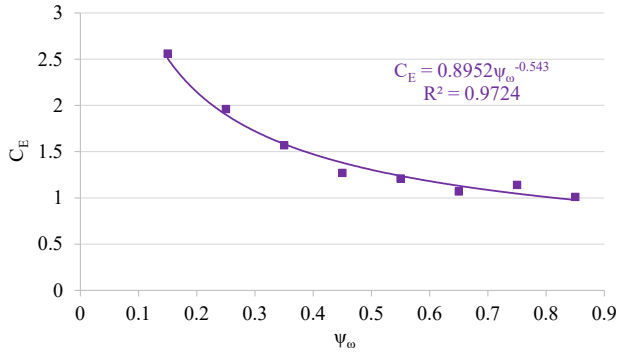

Fig. 6. Functional dependence of change in the total specific grinding efficiency C_E on the relative rotation speed ψ_ω

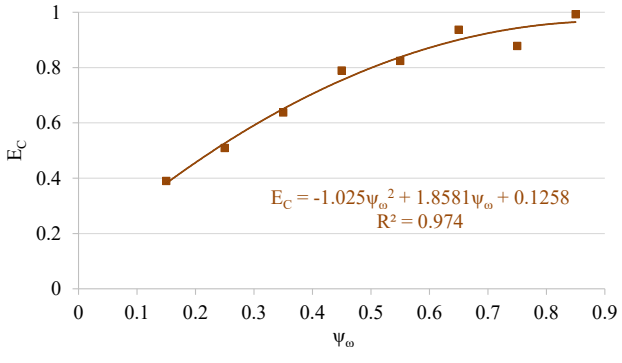

Fig. 7. Functional dependence of change in the total specific energy intensity of grinding E_C on the relative rotation speed ψ_ω

5. 4. Results of numerical modeling of the energy intensity of fill grinding processes by impact, crushing, and grinding mechanisms

Plots of our results from the numerical determination of change in the dimensionless parameters of the energy intensity of the grinding processes by impact, crushing, and grinding in a tumbling mill are shown in Fig. 8–12.

Plots of the results from the numerical determination of change in the mass fractions of the solid zone κ_{sr}, the shear layer zone κ_{sl}, and the flight zone κ_{fr} from the relative rotation speed ψ_ω are shown in Fig. 8. The values of κ_{sr}, κ_{sl} and κ_{fr} were calculated from expressions (7) to (9).

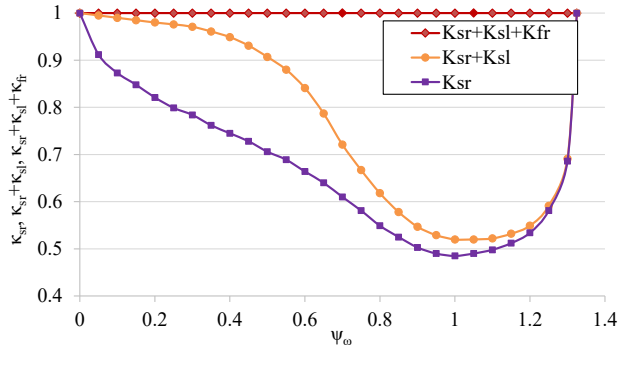

Fig. 8. Functional dependence of change in the mass fractions of the solid zone κ_{sr}, the shear layer zone κ_{sl}, and the flight zone κ_{fr} on the relative rotation speed ψ_ω

Plots of the results from numerical determination of the change in normalized analogs of the productivity of the processes of granulating by impact Q_{in}, crushing Q_{cn} and grinding Q_{an} depending on the relative rotation speed ψ_ω are shown in Fig. 9. The values of Q_{in}, Q_{cn} and Q_{an} were calculated using expressions (10) to (12).

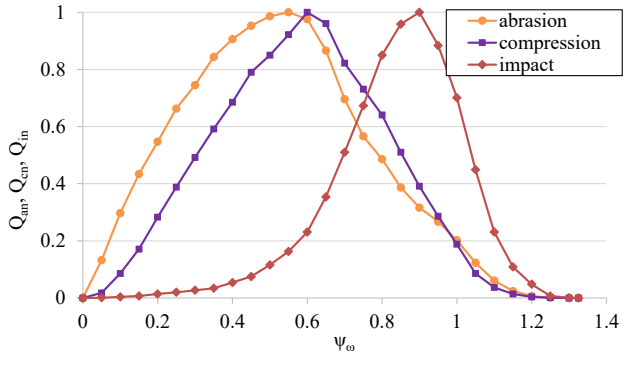

Fig. 9. Functional dependence of change in the normalized analogs of the productivity of the processes of granulating by impact Q_{in}, crushing Q_{cn}, and grinding Q_{an} on the relative rotation speed ψ_ω

Plots of our results from the numerical determination of change in the generalized analogs of the productivity of the processes of granulating by impact Q_{ig}, crushing Q_{cg}, and grinding Q_{ag} depending on the relative rotation speed ψ_ω are shown in Fig. 10. The Q_{ig}, Q_{cg} and Q_{ag} values were calculated using expressions (13) to (15).

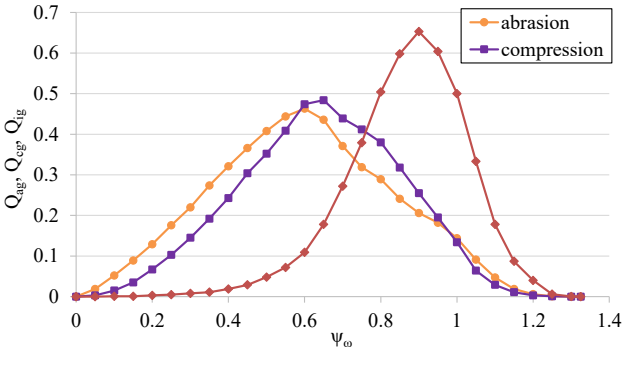

Fig. 10. Functional dependence of change in generalized analogs of the productivity of the processes of granulating by impact Q_{ig}, crushing Q_{cg}, and grinding Q_{ag} on the relative rotation speed ψ_ω

Plots of the results from the numerical determination of change in the analogs of the specific productivity of the processes of granulating by impact Q_{Ei}, crushing Q_{Ec}, and grinding Q_{Ea} depending on the relative rotation speed ψ_ω are shown in Fig. 11. The Q_{Ei}, Q_{Ec} and Q_{Ea} values were calculated from expressions (16) to (18).

Plots of our results from the numerical determination of change in the analogs of the specific energy intensity of the of granulating by impact E_{Qi}, crushing E_{Qc}, and grinding E_{Qa} from the relative rotation speed ψ_ω are shown in Fig. 12. The E_{Qi}, E_{Qc} and E_{Qa} values were calculated using expressions (19) to (21).

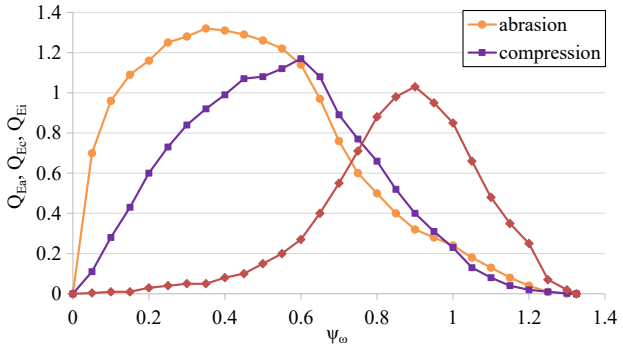

Fig. 11. Functional dependence of change in the specific productivity analogs of the processes of granulating by impact Q_{Ei}, crushing Q_{Ec}, and grinding Q_{Ea} on the relative rotation speed ψ_ω

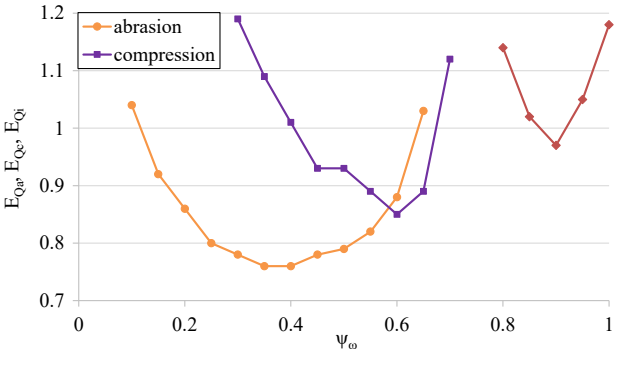

Fig. 12. Functional dependence of change in the specific energy intensity analogs of the processes of granulating by impact E_{Qi}, crushing E_{Qc}, and grinding E_{Qa} on the relative rotation speed ψ_ω

The obtained functional dependences of the numerical values of changes in dimensionless parameters of analytical modeling characterize the quantitative influence of rotation speed on the energy intensity of grinding processes in a tumbling mill for the mechanisms of destruction by impact, crushing, and grinding.

6. Results of investigating the energy efficiency of granulation processes in a tumbling mill by impact, crushing, and grinding: discussion and summary

Our results of experimental modeling have made it possible to assess the qualitative and quantitative influence of the rotation speed on the overall productivity of the grinding process in a tumbling mill. The algorithm of model calculations provided for the assessment of relative productivity by sieving through the control sieve C (2). A monotonic decrease in productivity with a decrease in rotation speed was found (Fig. 4). It was established that the relative productivity decreased by 2.9 times with a decrease in the relative rotation speed ψ_ω from 0.85 to 0.15. The revealed effect of speed on the overall productivity of the grinding process complements and expands similar results reported in [16–22].

The results of numerical modeling allowed us to assess the qualitative and quantitative influence of rotation speed on the energy intensity of the tumbling mill rotation drive. The algorithm of model calculations provided for the assessment of the energy intensity of the rotation drive by the

relative moment $\psi_{M0.5}$ (3) and the relative power $\psi_{P0.5}$ (4) of the resistance when the chamber is half filled with the load. A monotonic decrease in $\psi_{M0.5}$ and $\psi_{P0.5}$ with a decrease in the rotation speed was found (Fig. 5). It was established that $\psi_{M0.5}$ acquires a maximum value at $\psi_\omega = 0.85$, and $\psi_{P0.5}$ at $\psi_\omega = 0.9–0.95$. The revealed effect of speed on the energy intensity of the mill rotation drive complements and expands the data given in [10–14].

Our results of numerical simulation have made it possible to assess the qualitative influence of the rotation speed on the total energy intensity of the grinding process. The algorithm of model calculations provided for the assessment of the total energy intensity of the process by the total specific productivity C_E (5) and the total specific energy intensity E_C (6) of grinding, as the ratios of productivity C and the total power of the drive resistance $\psi_{P0.5}$. An intensive decrease in the energy intensity of grinding was found with a decrease in the rotation speed (Fig. 6, 7). The intensity of the decrease in energy intensity increases with a decrease in speed. It was found that the total specific productivity C_E (Fig. 6) increases and the total specific energy intensity E_C (Fig. 7) decreases by 2.5 times with a decrease in ψ_ω from 0.85 to 0.15. The revealed results on the influence of speed on the total energy intensity of the grinding process expand and complement the data reported in [15].

The results from numerical modeling allowed us to evaluate the comparative qualitative influence of the rotation speed on the energy intensity of the grinding process for the mechanisms of destruction of the crushed material by breaking, crushing and grinding. The algorithm of model calculations provided for the assessment of performance analogs for these mechanisms by the corresponding energies of impact Q_i, compression Q_c, and shear Q_a of the interaction of the loading elements [43–45].

The localization and intensity of the implementation of the interactions of the elements were determined by the zones of movement of the load in the cross-section of the rotating drum chamber. The implementation of the impact interaction is localized on the surface of the transition of the flight zone into the shear layer zone, the compression interaction – on the surface of the transition of the shear layer zone into the solid zone, the shear interaction – in the shear layer zone. The algorithm of model calculations provided for the assessment of the volumes of the zones of movement by the mass fractions of the solid zone κ_{sr} (7), the shear layer zone κ_{sl} (8), and the flight zone κ_{fr} (9). It was found that the minimum value of κ_{sr} and the maximum value of κ_{fr} were achieved at an increased rotation speed and the maximum value of κ_{sl} was achieved at a reduced speed (Fig. 8). It was found that the minimum value of κ_{sr} is 0.49 at $\psi_\omega = 1$, the maximum value of κ_{sl} is 0.2 at $\psi_\omega = 0.4–0.45$ and the maximum value of κ_{fr} is 0.48 at $\psi_\omega = 1–1.05$. The revealed effect of speed on the distribution of mass fractions of the loading motion zones clarifies and expands the similar results from [33–35].

The difference in the dimensionalities of values for productivity analogs Q_i, Q_c and Q_a discovered earlier in [43–45] caused inconveniences in conducting their comparative qualitative analysis. Therefore, the model calculation algorithm provided for further assessment of the values of the normalized productivity analogs of the processes of granulation by impact Q_{in} (10), crushing Q_{cn} (11), and grinding Q_{an} (12), as the ratios of their current and maximum values.

The next stage of the model calculation algorithm involved further comparative quantitative assessment of the identified analytical dependences of normalized productivity analogs Q_{in}, Q_{cn} and Q_{an} on rotation speed (Fig. 9), taking into account the proportional influence of the values of the experimentally obtained absolute productivity dependences on speed C (Fig. 4), by generalized productivity analogs of the processes of granulation by impact Q_{ig} (13), crushing Q_{cg} (14), and grinding Q_{ag} (15), as products of Q_{in}, Q_{cn} and Q_{an} and the total productivity C.

A monotonic sequential decrease was found, with a decrease in the rotation speed, of the maximum value of Q_{ig}, which is realized at an increased rotation speed, and the maximum values of Q_{cg} and Q_{ag}, which are realized at an average rotation speed (Fig. 10). It was found that the maximum value of Q_{ag}, which is realized at $\psi\omega = 0.6$, is 1.05 times inferior to the maximum value of Qcg, which is realized at $\psi_\omega = 0.65$, and 1.41 times inferior to the maximum value of Q_{ig}, which is realized at $\psi_\omega = 0.9$.

The results found on the influence of speed on the productivity of granulation processes by impact, crushing, and grinding coincide well with the data from GOST 10141-91 "Rod and ball mills. General technical requirements" and its analogs [46, 47]. These technical standards regulate the processes of wet grinding of ore and non-metallic minerals in tumbling mills. The extreme speed value found for impact grinding performance $\psi\omega = 0.9$ (Fig. 10) approaches the standard speed of ball mills $\psi\omega = 0.75–0.85$, which corresponds to the coarse grinding process mainly by impact. On the other hand, the extreme speed values found for crushing and grinding performance $\psi_\omega = 0.65$ and $\psi_\omega = 0.6$ (Fig. 10) approach the standard speed of rod mills with peripheral unloading $\psi_\omega = 0.55–0.65$, which corresponds to the medium grinding process mainly by grinding and crushing.

The final stage of the model calculation algorithm involved estimating the energy intensity of the grinding process in a tumbling mill when implementing individual loading mechanisms using the specific productivity analogs of the granulation processes by impact Q_{Ei} (16), crushing Q_{Ec} (17), and grinding Q_{Ea} (18) and the specific energy intensity analogs of the granulation processes by impact E_{Qi} (19), crushing E_{Qc} (20), and grinding E_{Qa} (21), as well as the ratios Q_{ig}, Q_{cg} and Q_{ag} and the relative power $\psi_{P0.5}$. An intensive decrease in the energy intensity of grinding with a decrease in the rotation speed was found (Fig. 11 and 12). The intensity of the decrease in energy intensity increases with a decrease in the speed. An intensive sequential increase, with a decrease in the rotation speed, of the maximum value of Q_{Ei}, realized at an increased rotation speed, the maximum value of Q_{Ec}, realized at an average speed, and the maximum value of Q_{Ea}, realized at a reduced speed (Fig. 11). It was found that the maximum value of Q_{Ea}, realized at $\psi_\omega = 0.35$, is 1.13 times greater than the maximum value of Q_{Ec}, realized at $\psi_\omega = 0.6$, and 1.28 times greater than the maximum value of QEi, realized at $\psi_\omega = 0.9$. An intensive sequential decrease, with a decrease in the rotation speed, of the minimum value of E_{Qi}, realized at an increased rotation speed, of the minimum value of E_{Qc}, realized at an average speed, and of the minimum value of Q_{Ei}, realized at a reduced speed (Fig. 12). It is established that the minimum value of E_{Qa}, which is realized at $\psi_\omega = 0.35$, is 1.13 times inferior to the minimum value of E_{Qc},, which is realized at $\psi_\omega = 0.6$, and 1.28 times inferior to the minimum value of E_{Qi}, which is realized at $\psi_\omega = 0.9$.

Analysis of Fig. 11, 12 reveals that the rational energy efficiency of the process of coarse grinding in a tumbling mill, mainly by impact, provided that unproductive contact of the loading flight zone with the cylindrical surface of the chamber is prevented, which reduces the grinding efficiency, can be considered an increased value of the rotation

speed $\psi_\omega = 0.75–0.9$. In this case, the value of the specific productivity of grinding by impact acquires a fraction of 0.69–1 of the maximum value. The rational energy efficiency of the process of medium grinding in a tumbling mill, mainly by crushing, can be considered an average speed value $\psi_\omega = 0.55–0.65$. In this case, the value of the specific productivity of grinding by crushing is 0.92–1 of the maximum value. The rational energy efficiency of the process of fine grinding in a tumbling mill, mainly by grinding, can be considered a reduced speed value $\psi_\omega = 0.3–0.4$. In this case, the specific productivity of grinding by grinding is 0.97–1 of the maximum value.

Comparative analysis has shown the convergence with the known data of the individual results obtained in determining the influence of rotation speed on the energy intensity of impact grinding, crushing and grinding. The identified values of specific productivity and energy intensity of grinding (Fig. 11, 12) supplement, expand, and refine similar results reported in [16–33] in terms of taking into account the influence of speed changes. The established extreme value of rotation speed $\psi_\omega = 0.9$ in terms of energy efficiency of the impact grinding process approaches the results from [16–22] in terms of identifying rational in terms of productivity increased values of speed $\psi_\omega = 0.7–0.85$. The identified extreme value of rotation speed $\psi_\omega = 0.6$ in terms of energy efficiency of the crushing grinding process approaches the results of papers [23–25] in terms of identifying rational in terms of energy intensity average values of speed $\psi_\omega = 0.55–0.6$. The extreme value of the rotational speed $\psi_\omega = 0.35$, which is found to be extremely efficient in terms of energy consumption, approaches the results reported in [26–30] on identifying rational, energy-efficient, reduced speed values $\psi_\omega = 0.3–0.4$. The results from [31–33] on identifying rational, energy-efficient, low speed values $\psi_\omega = 0.03–0.1$ correspond to the specific productivity of the grinding process by grinding, which is a fraction of 0.32–0.73 of the established maximum value (Fig. 11). It can be assumed that with a decrease in the degree of filling of the working chamber of the drum with the load, the further established speed value, which will correspond to achieving extreme energy efficiency of the process, will approach $\psi_\omega = 0.03–0.1$.

The results obtained in this work allow us to solve the problem of approximate modeling of the influence of rotation speed on the energy efficiency of grinding in a tumbling mill by impact, compression, and shear. The constructed numerical model made it possible to carry out a comparative analysis of the influence of speed on the destruction of the material by impact, crushing, and grinding during the implementation of the grinding process. This made it possible to predict an intensive decrease in the energy intensity of grinding with a decrease in rotation speed, as a defining characteristic of the process. Since granulation by impact, crushing, and grinding is related to the fineness of grinding, our model also makes it possible to predict the particle size composition of the final product of multi-stage disintegration.

The scope of application of the results is the implementation of stages of coarse, medium, and fine grinding of the multi-stage grinding process. The condition for using the results is an expedient change in the parameters of traditional working processes of tumbling mills. The potential expected effect of the use is to reduce the energy consumption of the grinding process by rationally changing the rotation speed, the degree of filling of the chamber and the content of the crushed material at different stages of the process.

The applicability of the established dynamic characteristics of the impact, compression, and shear interaction and the results of predicting the parameters of the coarse, medium, and fine grinding process by implementing the impact, crushing, and grinding mechanism is limited by the discrete values of the input parameters. The adopted value of the degree of filling of the drum chamber with the load was $\kappa = 0.45$, which corresponded to the grinding process in a tumbling mill with high throughput. The size of the granular particles of the model load relative to the diameter of the chamber was 0.0104.

The use of only the experimental method for physical visualization of the behavior of the internal chamber loading of the rotating drum by video recording through the transparent end wall of the chamber limited the accuracy of determining the velocity fields and boundaries of the zones of movement of granular particles. In the future, it is planned to search for opportunities to use X-ray systems to study the movement of granular media.

The disadvantage of this study is the use of one discrete value of the degree of filling, which imposes certain restrictions on the application of the results. It seems that a potentially interesting area of further research is to identify the characteristics of the interaction of elements with a different, in particular, smaller filling of the chamber with the load. This will make it possible to identify new dynamic effects of granulation mechanisms by impact, crushing, and grinding. In the future, it is advisable to experimentally determine the influence of the degree of filling of the chamber with the load on the technological and energy efficiency of grinding with the joint differentiated action of the mechanisms of loading by impact, compression, and shear. This will make it possible to establish rational conditions for the implementation of the mechanisms of destruction by breaking, crushing, and grinding when implementing energy-saving multi-stage grinding processes in grinding units with drum-type mills.

7. Conclusions

1. We have experimentally established that the productivity of the grinding process in a tumbling mill monotonically decreases with decreasing rotation speed. For the degree of filling the chamber with the load $\kappa = 0.45$, the relative productivity, estimated by the value of sieving through control sieve No. 008 at a grinding duration of 30 min, decreased by 2.9 times with a decrease in the relative rotation speed ψ_ω from 0.85 to 0.15.

2. It was experimentally established that the energy consumption of the tumbling mill rotation drive monotonically decreases with decreasing rotation speed. For $\kappa = 0.45$, the relative power of the load resistance to the rotation of the drum with a half-filling of the chamber $\psi_{P0.5}$ acquired a maximum value at $\psi_\omega = 0.9–0.95$.

3. Numerical modeling of the total energy intensity of the grinding process in a tumbling mill was based on the evaluation of the ratios of process productivity C and the power of the drive resistance to rotation $\psi_{P0.5}$. It was established that the total specific energy intensity of grinding decreases intensively with a decrease in the rotation speed. For $\kappa = 0.45$, with a decrease in ψ_ω from 0.85 to 0.15, the total specific productivity $C_E = C / \psi_{P0.5}$ increased and the total specific energy intensity $E_C = \psi_{P0.5} / C$ decreased by 2.5 times.

4. Numerical modeling of the energy intensity of grinding processes in a tumbling mill for impact, crushing, and grinding loading mechanisms was based on taking into account the relative dynamic parameters of impact, compression, and

shear interaction of granular elements. These interaction parameters are criteria for the similarity of the loading motion and the grinding process. The energies of the corresponding interactions were taken as analogs of the productivity of grinding processes. The energy intensity of grinding processes was estimated by the ratios of the analogs of the productivity of individual destruction mechanisms and the power of the drive resistance to rotation.

An intensive decrease in the energy intensity of grinding was revealed with a decrease in the rotation speed and a sequential transition of the prevailing loading mechanisms from high-speed impact to medium-speed crushing and low-speed grinding. For $\kappa = 0.45$, the maximum value of the specific productivity of the grinding process by grinding, which is realized at $\psi_\omega = 0.35$, is 1.13 times higher than the similar indicator of the grinding process by crushing, which is realized at $\psi_\omega = 0.6$, and is 1.28 times higher than this indicator of the grinding process by impact, which is realized at $\psi_\omega = 0.9$. The rational in terms of energy efficiency value of the speed for the coarse grinding process, mainly by impact, can be considered an increased $\psi_\omega = 0.75–0.9$, for medium grinding, mainly by crushing, the average $\psi_\omega = 0.55–0.65$, and for fine grinding, mainly by grinding, the reduced $\psi_\omega = 0.3–0.4$.

Conflicts of interest

The authors declare that they have no conflicts of interest in relation to the current study, including financial, personal, authorship, or any other, that could affect the study, as well as the results reported in this paper.

Funding

The study was conducted without financial support.

Data availability

All data are available, either in numerical or graphical form, in the main text of the manuscript.

Use of artificial intelligence

The authors confirm that they did not use artificial intelligence technologies when creating the current work.

References

1. Deniz, V. (2013). Comparisons of Dry Grinding Kinetics of Lignite, Bituminous Coal, and Petroleum Coke. Energy Sources, Part A: Recovery, Utilization, and Environmental Effects, 35 (10), 913–920. https://doi.org/10.1080/15567036.2010.514591
2. Góralczyk, M., Krot, P., Zimroz, R., Ogonowski, S. (2020). Increasing Energy Efficiency and Productivity of the Comminution Process in Tumbling Mills by Indirect Measurements of Internal Dynamics – An Overview. Energies, 13 (24), 6735. https://doi.org/10.3390/en13246735
3. Tavares, L. M. (2017). A Review of Advanced Ball Mill Modelling. KONA Powder and Particle Journal, 34, 106–124. https://doi.org/10.14356/kona.2017015
4. Kelly, E. G., Spottiswood, D. J. (1982). Introduction to Mineral Processing. Wiley.
5. Gupta, A., Yan, D. S. (Eds.) (2016). Mineral processing design and operations: An introduction. Elsevier. https://doi.org/10.1016/c2014-0-01236-1
6. King, R. P. (2001). Modeling and simulation of mineral processing systems. Elsevier. https://doi.org/10.1016/c2009-0-26303-3
7. Wills, B. A., Finch, J. (2015). Wills' mineral processing technology: an introduction to the practical aspects of ore treatment and mineral recovery. Butterworth-Heinemann. https://doi.org/10.1016/c2010-0-65478-2
8. Kwon, J., Jeong, J., Cho, H. (2016). Simulation and optimization of a two-stage ball mill grinding circuit of molybdenum ore. Advanced Powder Technology, 27 (4), 1073–1085. https://doi.org/10.1016/j.apt.2016.03.016
9. Dhiman, S., Joshi, R. S., Singh, S., Gill, S. S., Singh, H., Kumar, R., Kumar, V. (2022). Recycling of Ti6Al4V machining swarf into additive manufacturing feedstock powder to realise sustainable recycling goals. Journal of Cleaner Production, 348, 131342. https://doi.org/10.1016/j.jclepro.2022.131342
10. Mulenga, F. K., Moys, M. H. (2014). Effects of slurry filling and mill speed on the net power draw of a tumbling ball mill. Minerals Engineering, 56, 45–56. https://doi.org/10.1016/j.mineng.2013.10.028
11. Soleymani, M. M., Fooladi, M., Rezaeizadeh, M. (2016). Experimental investigation of the power draw of tumbling mills in wet grinding. Proceedings of the Institution of Mechanical Engineers, Part C: Journal of Mechanical Engineering Science, 230 (15), 2709–2719. https://doi.org/10.1177/0954406215598801
12. Soleymani, M. M., Fooladi, M., Rezaeizadeh, M. (2016). Effect of slurry pool formation on the load orientation, power draw, and impact force in tumbling mills. Powder Technology, 287, 160–168. https://doi.org/10.1016/j.powtec.2015.10.009
13. Yin, Z., Peng, Y., Zhu, Z., Ma, C., Yu, Z., Wu, G. (2019). Effect of mill speed and slurry filling on the charge dynamics by an instrumented ball. Advanced Powder Technology, 30 (8), 1611–1616. https://doi.org/10.1016/j.apt.2019.05.009
14. Bian, X., Wang, G., Wang, H., Wang, S., Lv, W. (2017). Effect of lifters and mill speed on particle behaviour, torque, and power consumption of a tumbling ball mill: Experimental study and DEM simulation. Minerals Engineering, 105, 22–35. https://doi.org/10.1016/j.mineng.2016.12.014
15. Anticoi, H., Guasch, E., Pérez-Álvarez, R., de Luis-Ruiz, J. M., Oliva, J., Hoffman Sampaio, C. (2022). Rod Mill Product Control and Its Relation to Energy Consumption: A Case Study. Minerals, 12 (2), 183. https://doi.org/10.3390/min12020183
16. Deniz, V. (2004). The effect of mill speed on kinetic breakage parameters of clinker and limestone. Cement and Concrete Research, 34 (8), 1365–1371. https://doi.org/10.1016/j.cemconres.2003.12.025

17. Deniz, V. (2013). Effects of Mill Speed on Kinetic Breakage Parameters of Four Different Particulate Pumices. Particulate Science and Technology, 31 (2), 101–108. https://doi.org/10.1080/02726351.2012.658903
18. Mulenga, F. K., Chimwani, N. (2013). Introduction to the use of the attainable region method in determining the optimal residence time of a ball mill. International Journal of Mineral Processing, 125, 39–50. https://doi.org/10.1016/j.minpro.2013.09.007
19. Yin, Z., Peng, Y., Zhu, Z., Yu, Z., Li, T. (2017). Impact Load Behavior between Different Charge and Lifter in a Laboratory-Scale Mill. Materials, 10 (8), 882. https://doi.org/10.3390/ma10080882
20. Soleymani, M. M. (2021). RETRACTED: Experimental Study of Operational Parameters on Product Size Distribution of Tumbling Mill. Proceedings of the Institution of Mechanical Engineers, Part E: Journal of Process Mechanical Engineering. https://doi.org/10.1177/09544089211062763
21. Li, T., Yin, Z., Wu, G. (2021). Study on heat transfer behavior and thermal breakage characteristic of the charge in ball mills. Advances in Mechanical Engineering, 13 (3). https://doi.org/10.1177/1687814021994964
22. Cayirli, S. (2018). Influences of operating parameters on dry ball mill performance. Physicochemical Problems of Mineral Processing, 54 (3). https://doi.org/10.5277/ppmp1876
23. Hanumanthappa, H., Vardhan, H., Mandela, G. R., Kaza, M., Sah, R., Shanmugam, B. K. (2020). A comparative study on a newly designed ball mill and the conventional ball mill performance with respect to the particle size distribution and recirculating load at the discharge end. Minerals Engineering, 145, 106091. https://doi.org/10.1016/j.mineng.2019.106091
24. Gupta, V. K., Sharma, S. (2014). Analysis of ball mill grinding operation using mill power specific kinetic parameters. Advanced Powder Technology, 25 (2), 625–634. https://doi.org/10.1016/j.apt.2013.10.003
25. Gupta, V. K. (2020). Energy absorption and specific breakage rate of particles under different operating conditions in dry ball milling. Powder Technology, 361, 827–835. https://doi.org/10.1016/j.powtec.2019.11.033
26. Chimwani, N., Mulenga, F. K., Hildebrandt, D., Glasser, D., Bwalya, M. M. (2014). Scale-up of batch grinding data for simulation of industrial milling of platinum group minerals ore. Minerals Engineering, 63, 100–109. https://doi.org/10.1016/j.mineng.2014.01.023
27. Chimwani, N., Mulenga, F. K., Hildebrandt, D., Glasser, D., Bwalya, M. M. (2015). Use of the attainable region method to simulate a full-scale ball mill with a realistic transport model. Minerals Engineering, 73, 116–123. https://doi.org/10.1016/j.mineng.2014.06.012
28. Chimwani, N., Hildebrandt, D. (2018). Modeling of an open mill with scalped feed for the maximum production of a desired particle size range. Particulate Science and Technology, 37 (3), 314–324. https://doi.org/10.1080/02726351.2017.1370048
29. Chimwani, N. (2021). A Review of the Milestones Reached by the Attainable Region Optimisation Technique in Particle Size Reduction. Minerals, 11 (11), 1280. https://doi.org/10.3390/min11111280
30. Makgoale, D. M. (2019). Effects Of Mill Rotational Speed On The Batch Grinding Kinetics Of A UG2 Platinum Ore. UNISA. Available at: https://uir.unisa.ac.za/items/2894bd6d-32c1-418e-a4c5-e011f4b757d0
31. Metzger, M. J., Glasser, B. J. (2013). Simulation of the breakage of bonded agglomerates in a ball mill. Powder Technology, 237, 286–302. https://doi.org/10.1016/j.powtec.2012.12.006
32. Metzger, M. J., Desai, S. P., Glasser, D., Hildebrandt, D., Glasser, B. J. (2011). Using the attainable region analysis to determine the effect of process parameters on breakage in a ball mill. AIChE Journal, 58 (9), 2665–2673. https://doi.org/10.1002/aic.12792
33. Metzger, M. J., Glasser, D., Hausberger, B., Hildebrandt, D., Glasser, B. J. (2009). Use of the attainable region analysis to optimize particle breakage in a ball mill. Chemical Engineering Science, 64 (17), 3766–3777. https://doi.org/10.1016/j.ces.2009.05.012
34. Naumenko, Y. (2017). Modeling of fracture surface of the quasi solid-body zone of motion of the granular fill in a rotating chamber. Eastern-European Journal of Enterprise Technologies, 2 (1 (86)), 50–57. https://doi.org/10.15587/1729-4061.2017.96447
35. Naumenko, Y., Sivko, V. (2017). The rotating chamber granular fill shear layer flow simulation. Eastern-European Journal of Enterprise Technologies, 4 (7 (88)), 57–64. https://doi.org/10.15587/1729-4061.2017.107242
36. Naumenko, Y. (2017). Modeling a flow pattern of the granular fill in the cross section of a rotating chamber. Eastern-European Journal of Enterprise Technologies, 5 (1 (89)), 59–69. https://doi.org/10.15587/1729-4061.2017.110444
37. Deineka, K., Naumenko, Y. (2019). Revealing the effect of decreased energy intensity of grinding in a tumbling mill during self-excitation of auto-oscillations of the intrachamber fill. Eastern-European Journal of Enterprise Technologies, 1 (1), 6–15. https://doi.org/10.15587/1729-4061.2019.155461
38. Deineka, K., Naumenko, Y. (2019). Establishing the effect of a decrease in power intensity of self-oscillating grinding in a tumbling mill with a reduction in an intrachamber fill. Eastern-European Journal of Enterprise Technologies, 6 (7 (102)), 43–52. https://doi.org/10.15587/1729-4061.2019.183291
39. Deineka, K., Naumenko, Y. (2020). Establishing the effect of decreased power intensity of self-oscillatory grinding in a tumbling mill when the crushed material content in the intra-chamber fill is reduced. Eastern-European Journal of Enterprise Technologies, 4 (1 (106)), 39–48. https://doi.org/10.15587/1729-4061.2020.209050
40. Deineka, K., Naumenko, Y. (2021). Establishing the effect of a simultaneous reduction in the filling load inside a chamber and in the content of the crushed material on the energy intensity of self-oscillatory grinding in a tumbling mill. Eastern-European Journal of Enterprise Technologies, 1 (1 (109)), 77–87. https://doi.org/10.15587/1729-4061.2021.224948
41. Deineka, K., Naumenko, Y. (2022). Revealing the mechanism of stability loss of a two-fraction granular flow in a rotating drum. Eastern-European Journal of Enterprise Technologies, 4 (1 (118)), 34–46. https://doi.org/10.15587/1729-4061.2022.263097
42. Deineka, K. Yu., Naumenko, Yu. V. (2018). The tumbling mill rotation stability. Scientific Bulletin of National Mining University, 1, 60–68. https://doi.org/10.29202/nvngu/2018-1/10

43. Naumenko, Y., Deineka, K. (2023). Building a model of the impact grinding mechanism in a tumbling mill based on data visualization. Eastern-European Journal of Enterprise Technologies, 3 (7 (123)), 65–73. https://doi.org/10.15587/1729-4061.2023.283073
44. Naumenko, Y., Deineka, K. (2023). Building a model of the compression grinding mechanism in a tumbling mill based on data visualization. Eastern-European Journal of Enterprise Technologies, 5 (1 (125)), 64–72. https://doi.org/10.15587/1729-4061.2023.287565
45. Naumenko, Y., Deineka, K., Zabchyk, S. (2024). Building a model of the abrasion grinding mechanism in a tumbling mill based on data visualization. Eastern-European Journal of Enterprise Technologies, 2 (1 (128)), 21–33. https://doi.org/10.15587/1729-4061.2024.301653
46. Coal preparation plant – Principles and conventions for flowsheets (ISO/IEC Standard No. 924:1989). International Organization for Standardization. Available at: https://www.iso.org/ru/standard/5340.html
47. DIN EN 1009-3. Maschinen für die mechanische Aufbereitung von Mineralien und ähnlichen festen Stoffen – Sicherheit – Teil 3: Spezifische Anforderungen für Brecher und Mühlen; Deutsche Fassung EN 1009-3:2020. Deutsches Institut für Normung. Available at: https://www.din.de/de/mitwirken/normenausschuesse/nam/veroeffentlichungen/wdc-beuth:din21:316006092